



PCCP

## Halogen and Structure Sensitivity of Halobenzene Adsorption on Copper Surfaces

Journal:	<i>Physical Chemistry Chemical Physics</i>
Manuscript ID	CP-ART-12-2021-005660
Article Type:	Paper
Date Submitted by the Author:	11-Dec-2021
Complete List of Authors:	Schunke, Christina; Ruhr-Universität Bochum, Miller, Daniel; Hofstra University, Chemistry Zurek, Eva; SUNY at Buffalo, Chemistry Morgenstern, Karina; Ruhr-Universität Bochum, Chemistry and Biochemistry

SCHOLARONE™  
Manuscripts

## ARTICLE

## Halogen and Structure Sensitivity of Halobenzene Adsorption on Copper Surfaces †

Christina Schunke<sup>\*a</sup>, Daniel P. Miller<sup>b</sup>, Eva Zurek<sup>c</sup>, and Karina Morgenstern<sup>a</sup>Received 00th January 20xx,  
Accepted 00th January 20xx

DOI: 10.1039/x0xx00000x

The adsorption orientation of molecules on surfaces influences their reactivity, but it is still challenging to tailor the interactions that govern their orientation. Here, we investigate how the substituent and the surface structure alter the adsorption orientation of halogenated benzene molecules from parallel to tilted relative to the surface plane. The deviation of the parallel orientation of bromo-, chloro-, and fluorobenzene molecules adsorbed on Cu(111) and Cu(110) surfaces is determined, utilising the surface selection rule in reflection-absorption infrared spectroscopy. On Cu(111), all three halogenated molecules are adsorbed with their molecular plane almost parallel to the surface at low coverages. However, they are tilted at higher coverages; yet, the threshold coverages differ. On Cu(110), merely bromo- and chlorobenzene follow this trend, albeit with a lower threshold for both. In contrast, fluorobenzene molecules are tilted already at low coverages. The substantial influence of the halogen atom and the surface structure on the adsorption orientation, resulting from an interplay of molecule-molecule and molecule-surface interactions, is highly relevant for reactivity confined to two dimensions.

### Introduction

Reactions in confined geometries are limited or promoted by the bonds made available by the confinement-induced orientation of the reactants<sup>1</sup>. Predicting reaction efficiencies in the two-dimensional confinement on surfaces thus demands a thorough knowledge about the adsorption orientations of the participating molecules<sup>2,3</sup>. This should be particularly true for the emerging field of on-surface synthesis on metal surfaces, which investigates individually synthesised molecules by scanning tunnelling microscopy<sup>4,5</sup>. The first<sup>6,7</sup> and still most prominently employed<sup>8,9</sup> path in on-surface synthesis uses Ullmann-like coupling<sup>10</sup>, a C-C-coupling from halogenated molecules on the coinage metal surfaces<sup>11,12</sup>. So far, its reaction efficiency was mainly tuned by precursor design<sup>6,13</sup> and the choice of the substrate material<sup>13,14,15</sup>. Other parameters as the surface structure, the halogen type, or the resulting adsorbate orientation<sup>16</sup> have not yet been explored systematically, though the particular importance of the

adsorption orientation has been demonstrated recently for another reaction<sup>17</sup>.

So far, only one study has determined a high-coverage adsorption orientation for the halogenated molecules that participate in Ullmann coupling<sup>18</sup>. At the one coverage of 0.8 ML explored, iodo- and bromobenzene both adsorb on Cu(111) at a tilt angle of 45° relative to the surface normal, a coincidence as we will show in this article. The parent molecule and building block of all aromatic compounds, benzene, demonstrated the complexity of adsorption orientation<sup>19,20,21</sup>. On Cu(111) benzene adsorbs parallel to the surface at all coverages<sup>21</sup>, on Pd(111) it adsorbs tilted already at lower coverage<sup>19</sup>, and on Cu(100) it adsorbs tilted only at higher coverage<sup>20</sup>. Based on density functional theory, a calculated tilt on Cu(100) in a small simulation cell was explained by a repulsive interaction between the adsorbed benzene molecules<sup>20</sup>. For another molecule that is not of relevance in on-surface synthesis, acetophenone, infrared spectroscopy demonstrated recently that only the additionally adsorbed molecules are tilted, while the initially-adsorbed molecules remain in their parallel adsorption orientation<sup>22</sup>. This method does not determine the exact tilt angle but allows a qualitative determination of changes to the adsorption orientation. For a larger molecule, astraphloxin, the coverage even induces a conformational selectivity<sup>23</sup>.

In general, the orientation of the adsorbate results from the subtle interplay of surface-molecule and molecule-molecule interactions as well established for, e.g., self-assembled monolayers<sup>24</sup> or water structures<sup>25</sup>. For the halogenated molecules that participate in the Ullmann coupling, the

<sup>a</sup> Ruhr-Universität Bochum, Lehrstuhl für Physikalische Chemie I, Universitätsstraße 150, D-44803 Bochum, Germany.

<sup>b</sup> Hofstra University, Department of Chemistry, 106 Berliner Hall, Hempstead, NY 11549, U.S.A.

<sup>c</sup> State University of New York at Buffalo, Department of Chemistry, 777 Natural Sciences Complex, Buffalo, NY 14260-3000, U.S.A.

† Electronic Supplementary Information (ESI) available: This supplementary information provides LEED pattern and STM images to prove the cleanliness of the surface prior to molecule adsorption. Furthermore, the calibration of the coverage is described based on TPD spectra. The full-range spectra and calculated IR spectra are presented. The computational details, discussion, figures, and data for DFT calculations are provided. See DOI: 10.1039/x0xx00000x

molecule-molecule interactions comprise weak hydrogen bonds and halogen bonds<sup>26,27</sup>. Both bonds are directional non-covalent interactions. While hydrogen bonds are strongest at an angle of 180°, halogen bonds are strongest at a 90° angle for the C-X bonds of adjacent molecules (X: chlorine, bromine, or iodine)<sup>28</sup>. This angle results from a charge redistribution at the halogen upon C-X formation, leading to a belt-shaped maximum perpendicular to the C-X bond at the halogen atom and a minimum at the far end of the halogen atom along the C-X bond - a so-called  $\sigma$ -hole<sup>28</sup>. The size of the  $\sigma$ -hole and its bond strength increases with decreasing electronegativity of the halogen<sup>29</sup>. The influence of the surface-molecule interaction on the strength and the directionality of halogen bonds were investigated recently at low coverages<sup>30</sup>, but not yet its influence on adsorption orientation.

In this article, we explore the coverage-dependent qualitative adsorption orientation of bromo-, chloro-, and fluorobenzene on two Cu surfaces. The substituted benzene molecules form the building blocks for those molecules employed in on-surface synthesis involving Ullmann coupling. We compare their adsorption orientation on the two low-index surfaces, which differ most concerning the surface corrugation. The hexagonal (111) surface is hardly corrugated for many large molecules, being the closest surface to a simple plane. On the other hand, the rectangular (110) surface is highly corrugated with well-separated rows. On these surfaces, we determine at which coverages the molecules alter their orientation from parallel to tilted via reflection-absorption infrared spectroscopy (RAIRS); employing the surface selection rule<sup>31</sup>. The coverage dependence of the six systems is surprisingly diverse. We discuss the influence of molecule-molecule and molecule-substrate interactions on their coverage-dependent orientations.

## Experimental Section

The experiments were performed with an infrared (IR) spectrometer under ultra-high vacuum (UHV) conditions at a base pressure of  $2 \cdot 10^{-10}$  mbar<sup>32</sup>.

The reflection-absorption infrared spectroscopy (RAIRS) spectra are obtained using a Fourier transform infrared (FTIR) spectrometer (*Bruker Vertex 80v*) with  $4 \text{ cm}^{-1}$  resolution; equipped with a thermal light source (globar), an UltraScan interferometer (optical resolution  $< 0.2 \text{ cm}^{-1}$ ), and a nitrogen-cooled mercury cadmium telluride (MCT) detector, which offers a spectral range of  $4000 \text{ cm}^{-1}$  to  $800 \text{ cm}^{-1}$ . The IR beam is guided through differentially pumped KBr windows to the sample. Each IR spectrum represents an average of 400 spectra. With this procedure, the detection limit is 0.2 ML. Featureless regions of the spectra are cut out for better visibility of the other regions.

Refer to the supplementary information (ESI) for the complete spectra. The areas of the peaks are determined via Gaussian fits, whereby the width is set to the same value for all peaks.

The relative adsorption orientation to the surface of the molecules is determined from the spectra employing the surface selection rule for molecules adsorbed on a metal

surface<sup>31</sup>. According to this rule, only those vibrational modes contribute to the spectra, which have a component of their oscillating dipole moment perpendicular to the surface. Dipoles that are oscillating parallel to the surface do not contribute. In benzene molecules, the C-C stretching vibrations are such vibrations within the molecular plane that are not visible if the molecule adsorbs with its molecular plane parallel to the surface plane. The method determines whether a mode vibrates in parallel or not but it does not deliver adsorption angles.

The single crystalline Cu(111) and Cu(110) samples are cleaned by standard cycles of sputtering for 30 min with  $\text{Ar}^+$  ions at 1.3 keV for Cu(111) and 0.6 keV for Cu(110) ( $I_{\text{sputter}} = 10 \mu\text{A}$ ) and annealing at 850 K for 20 min. LEED pattern and STM images support the cleanliness of the surface (see ESI, section S1). Bromo-, chloro-, and fluorobenzene molecules (*Merck*) are filled into glass crucibles, attached to a separately pumped UHV chamber named molecule deposition chamber. The molecules are degassed to remove residual impurities by freeze-pump-thaw cycles. At room temperature, the vapour pressure of all molecules is sufficient for deposition. A pressure of  $5 \cdot 10^{-7}$  mbar is set within the molecule deposition chamber via a leak valve from this vapour pressure.

Then, the molecules are introduced into the main chamber through a gate-through valve, which opens towards the surface.

They are deposited for 20 s to 180 s onto the surface held at 110 K. As the pressure at the sample is around two orders of magnitude lower than that set in the molecule deposition chamber before opening the valve, the resulting coverages are between 0.25 ML and 2.25 ML (monolayers). These coverages are calibrated based on features in temperature-programmed desorption (TPD, see ESI, section S2) data. The definition of one monolayer refers to an earlier convention used in literature based on TPD data of benzene on Cu(111)<sup>21</sup>. The highest density for parallel adsorbed molecules, considering their van-der-Waals radii, is 1.5 molecules per  $\text{nm}^{-2}$ , corresponding to 1.5 ML according to this definition. The computational details, discussion, figures, and data for DFT calculations performed on the halobenzenes are given in the ESI in section S4.

## Results

### Influence of halogen substituent on multilayer spectra

This article aims to analyse whether or not a molecule is adsorbed in parallel to the surface plane, called adsorption orientation.

Before studying the influence of coverage and surface structure on the adsorption orientation, we recapitulate how the halogen substituents alter the vibrational spectra based on a spectrum for molecules adsorbed on Cu(110) at the high coverage of 2 ML (Fig. 1). For the specific definition of 1 ML for halogenated benzene molecules, see the experimental section. At this high coverage, a negligible influence of the surface structure is expected. Indeed, the wave numbers of the

vibrational modes of the investigated halobenzene molecules match the literature values measured in gas-phase<sup>33</sup> within our experimental precision. Furthermore, the DFT vibrational frequencies are in good agreement with the experimental RAIRS in both wavenumber, intensity, assignment, and character (see ESI, section S4). We concentrate here on the

with the experimental wave numbers. The C-C stretching vibrations of the benzene

Tab. 1 Comparison of measured vibrational modes (meas.) of bromo (PhBr)-, chloro (PhCl)-, and fluorobenzene (PhF) at 2 ML on Cu(110) to literature (lit.) gas-phase values<sup>33</sup>.

vibration (cm <sup>-1</sup> )		PhBr	PhCl	PhF
ν(C-X)	meas.	1070	1084, 1078	1222
	lit.	1070,	1084	1219
ν(C-C)	meas.	1473	1478	1487
	lit.	1473	1477	1492
ν(C-C)	meas.	1441	1444	1458
	lit.	1445	1445	-
β(C-H)	meas.	-	1068	1066
	lit.	-	1068	1065
β(C-H)	meas.	1018	1022	1022
	lit.	1021	1026	1020

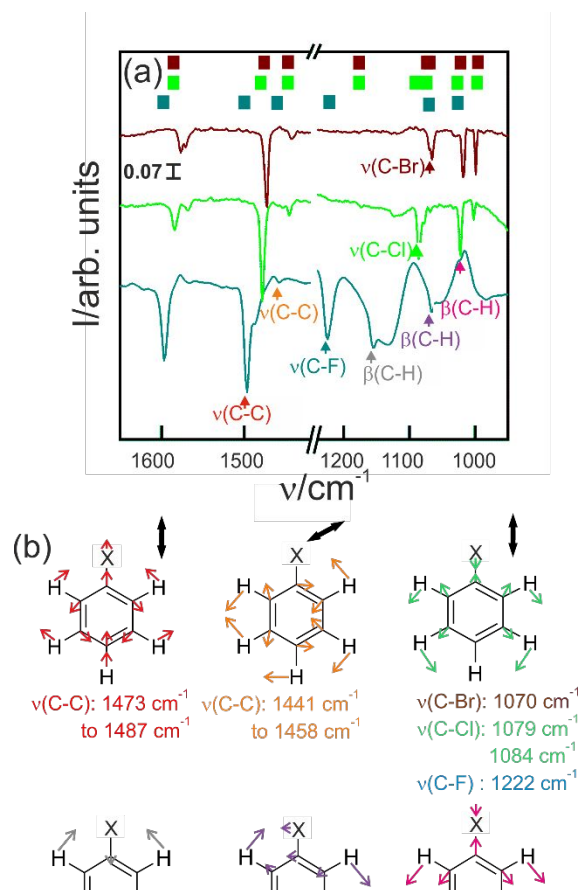


Fig. 1 Dependence of the vibrational modes of halobenzene on the halogen substituent for 2 ML on Cu(110): (a) RAIR spectra of bromo- (brown), chloro- (green), and fluorobenzene (blue) molecules. C-C stretching vibrations are marked in red and orange (1500-1400 cm<sup>-1</sup> C-H deformation vibrations in purple and pink (1200-1000 cm<sup>-1</sup>), and C-X stretching vibrations in brown for X = Br (1070 cm<sup>-1</sup>), green for X = Cl (1084 cm<sup>-1</sup> and 1078 cm<sup>-1</sup>), and blue for X = F (1222 cm<sup>-1</sup>). Coloured bars on the top mark the gas-phase vibrational modes in the same colour as the spectra<sup>33</sup>. (b) Schemes of vibrational modes in the same colour as in (a) with their wave numbers. Double arrows in the top row indicate the change in dipole moment.

most intense vibrational modes in the spectra as marked in Fig. 1a and listed in Tab. 1.

The positions of the most intense vibrational modes depend on the nature of the halogen, most prominently for the C-X stretching vibrations. The difference of  $\Delta\nu = 138$  cm<sup>-1</sup> (DFT 128 cm<sup>-1</sup>) between 1084 cm<sup>-1</sup> and 1222 cm<sup>-1</sup> for C-Cl (marked in green) and C-F (blue), respectively, is considerably larger than the  $\Delta\nu = 14$  cm<sup>-1</sup> (DFT 17 cm<sup>-1</sup>) between C-Cl (1084 cm<sup>-1</sup>) and C-Br (1070 cm<sup>-1</sup>, brown). The DFT vibrational frequencies found the C-F, C-Cl, and C-Br vibrations to occur at 1187/1225 cm<sup>-1</sup>, 1059/1065 cm<sup>-1</sup>, and 1042/1048 cm<sup>-1</sup> using revPBE-D3/ $\omega$ B97X-D, respectively, being in good agreement

rings (red and orange) are affected little. Their difference is again more pronounced between fluorobenzene and chlorobenzene, at  $\Delta\nu = 12$  cm<sup>-1</sup> (orange) and  $\Delta\nu = 25$  cm<sup>-1</sup> (red) than between bromo- and chlorobenzene ( $\Delta\nu = 5$  cm<sup>-1</sup>). In contrast to the C-C and C-X stretching vibrations, the C-H deformation vibrations are at 1066 cm<sup>-1</sup> (purple) and 1022 cm<sup>-1</sup> (pink), independent from the substituent. All wave numbers of the vibrational modes are identical to the gas-phase values within the experimental error for all halogen substituents (cf. Tab. 1). Other than reported in the literature, the C-Cl stretching vibration consists of two maxima at 1084 cm<sup>-1</sup> and 1078 cm<sup>-1</sup>, a splitting that does not exist for the C-Br and C-F stretching vibrations (Fig. 1a). The area ratio of these two peaks corresponds, at 30 % (at 1078 cm<sup>-1</sup>) to 70 % (at 1084 cm<sup>-1</sup>) to the natural isotope ratio of <sup>37</sup>Cl and <sup>35</sup>Cl. As neither bromine nor fluorine has a natural isotope at a similar large abundance, no double-peak structure is expected, as observed experimentally.

The halogen substituent influences not only the wave numbers but also the intensity of the modes. The most significant intensity difference of the C-H deformation vibration at 1022 cm<sup>-1</sup> is seven times higher for fluorobenzene than for bromo- or chlorobenzene. Such differences in intensity are related to the different dipole gradients, which influence the signal intensity in IR spectroscopy<sup>34</sup>. The agreement between the measured RAIRS, literature gas-phase, and DFT computed spectra confirm that the surface has no measurable influence on the vibrational modes at a coverage of 2.00 ML within the accuracy of our measurement (4 cm<sup>-1</sup>).

### Influence of the surface structure on the adsorption orientation

Having recapitulated the influence of the halogen substituent on the vibrational modes of halogenated benzene molecules, we now investigate how the surface structure influences their adsorption orientation. As the wave numbers of the vibrational modes are independent of coverage for all surface-molecule combinations, we concentrate on their intensities. For this aim, we compare the coverage dependence of the vibrational modes of the three substituted benzene molecules

on Cu(111) to those on Cu(110), starting with bromobenzene (Fig. 2). We determine the adsorption orientation using the vibrational modes marked in Fig. 2a. These are the C-C stretching vibrations at  $1473\text{ cm}^{-1}$

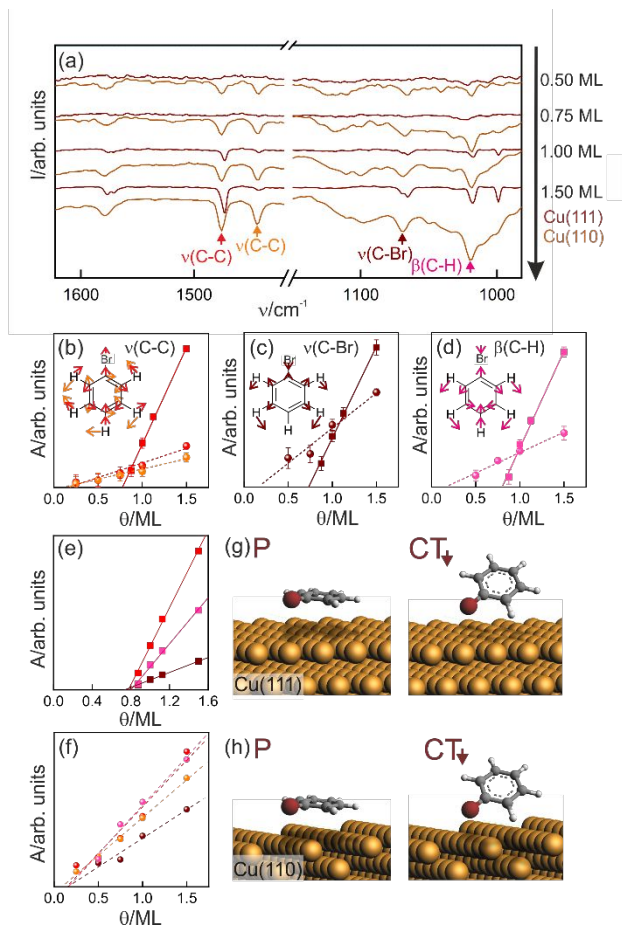


Fig. 2 Dependence of the adsorption orientation of bromobenzene on surface structure: (a) RAIR spectra of bromobenzene molecules on Cu(111) (darker brown) and Cu(110) (lighter brown). The coverage increases from top to bottom (0.25 ML, 0.50 ML, 0.75 ML, 1.00 ML, 1.50 ML); see ESI, section S3, for the complete spectra. Marked vibrations are shown in the insets of the panels (b) to (d), arrows point to the direction of motion. (b-f) Peak area  $A$  versus coverage  $\theta$  for (b) C-C stretching vibrations at  $1477\text{ cm}^{-1}$  (red) and  $1444\text{ cm}^{-1}$  (orange), (c) C-Br stretching vibration at  $1070\text{ cm}^{-1}$  (brown), and (d) C-H deformation vibration at  $1022\text{ cm}^{-1}$  (pink). The solid and dashed lines on (e) Cu(111) (squares) and (f) Cu(110) (circles) are linear fits to the data. Colours correspond to vibrational modes marked in (a). (g, h) Scheme of the different adsorption orientations on (g) Cu(111) and (h) Cu(110) with P for parallel and  $\text{CT}_{\downarrow}$  for completely tilted adsorption orientation. Note that the pictured angles of the molecules do not represent exact values.

(red) and  $1441\text{ cm}^{-1}$  (orange), which mainly indicate the orientation of the benzene ring. Thereby, the vibrational mode at  $1441\text{ cm}^{-1}$  is not considered on Cu(111) because of its low intensity. The C-Br stretching vibration at  $1070\text{ cm}^{-1}$  (brown) indicates the orientation of the C-Br bond and the C-H deformation vibration at  $1018\text{ cm}^{-1}$  (pink) that of the C-H bonds. If the C-H bonds remained in the molecular plane upon adsorption, the latter would likewise indicate the adsorption orientation of the ring. Otherwise, it suggests an out-of-plane bending of the C-H bonds.

The spectra differ for some coverages at which vibrational modes visible in the Cu(110) spectra do not exist in those on Cu(111). For example, the C-C stretching vibrations (red and orange) are detectable at 0.50 ML on Cu(110) but not on Cu(111) (Fig. 2a, lighter brown vs darker brown). We quantify this difference via the coverage dependence of the peak areas. These areas rise linearly with coverage above a threshold for all modes (Fig. 2b-d). Such a linear increase indicates that molecules below the thresholds are adsorbed with their vibrations parallel to the surface. In contrast, additional molecules adsorb in a tilted adsorption orientation to this vibration, contrasting an adsorption mode in which already adsorbed molecules change their adsorption orientation at higher coverage resulting in a non-linear coverage dependence (see below).

For both surfaces, all intersections of the fits with the x-axes fall into the same range but differ between the surfaces (Fig. 2e, f). They vary between 0.73 and 0.79 ML for Cu(111) (Fig. 2e) and between 0.13 and 0.20 ML for Cu(110) (Fig. 2f), at averages of  $(0.77 \pm 0.03)\text{ ML}$  and  $(0.17 \pm 0.02)\text{ ML}$  for Cu(111) and Cu(110), respectively. Thus, almost five times as many bromobenzene molecules adsorb parallel to Cu(110) than to Cu(111), a major influence of the different surface structures. Above the thresholds, all modes are visible, implying that all vibrations, the ring, C-X, and C-H, oscillate with some component perpendicular to the surface. We name this adsorption orientation completely tilted with the halogen pointing towards the surface (Fig. 2g, h,  $\text{CT}_{\downarrow}$ ).

To investigate the influence of the halogen atom on the adsorption orientation, we now turn to chlorobenzene (Fig. 3). Also, for chlorobenzene, the positions of the vibrational modes are independent of coverage on both surfaces. In addition to the vibrational modes analysed for bromobenzene, the C-H deformation vibration at  $1068\text{ cm}^{-1}$  (in purple) confirms the orientations of the C-H bonds as inferred from the other C-H deformation vibrations. As for bromobenzene, the areas of the vibrational peaks increase linearly with coverage. For Cu(111), the linear fits intersect the x-axes in a region between 0.49 and 0.60 ML, at an average threshold of  $(0.56 \pm 0.02)\text{ ML}$  (Fig. 3 b-d). Thus, the threshold for a tilted orientation of additionally adsorbed molecules is at a smaller coverage for chlorobenzene than for bromobenzene, i.e., fewer molecules adsorb in a parallel adsorption orientation.

On Cu(110), the spread of the intersections is so broad that no common point of intersection exists (Fig. 3f). Instead, there are two regions of common intersections, one at  $(0.12 \pm 0.01)\text{ ML}$  and one at  $(0.37 \pm 0.02)\text{ ML}$  (Fig. 3f, inset).<sup>5</sup> These two thresholds point to two distinct tilted adsorption orientations, depicted in Fig. 3h as PT and  $\text{CT}_{\downarrow}$ . The detectability of the C-Cl stretching vibration only above the second threshold indicates that the C-Cl bond remains in parallel to the surface up to this coverage (Fig. 3c, green). The molecules are thus tilted around this bond between the thresholds, explaining the detectability of the two C-H deformation vibrations (Fig. 3d, purple and pink) and C-C stretching vibrations at  $1444\text{ cm}^{-1}$  (Fig. 3b, orange). We name this adsorption orientation partially tilted (Fig. 3h, PT). The

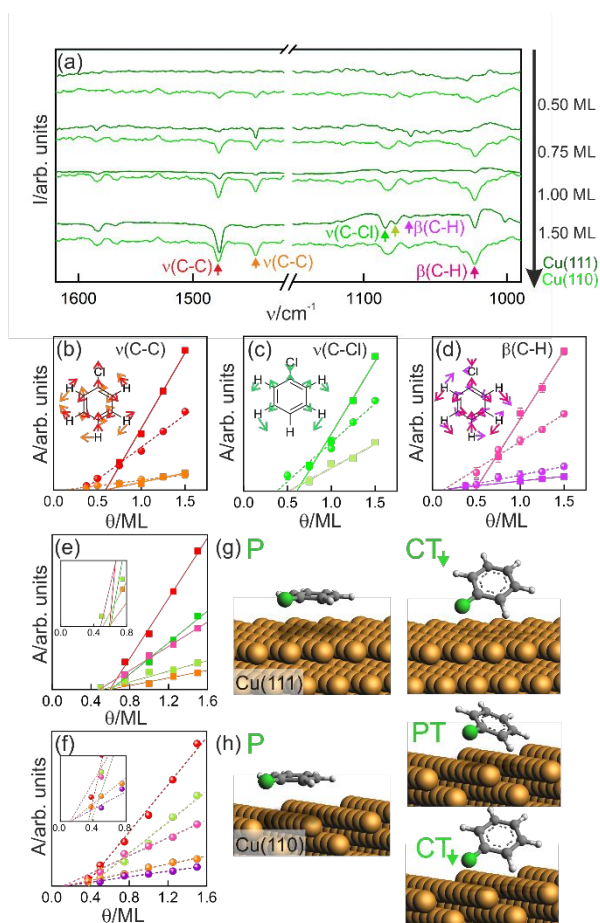


Fig. 3 Dependence of the adsorption orientation of chlorobenzene on surface structure: (a) RAIR spectra of chlorobenzene molecules on Cu(111) (darker green) and Cu(110) (lighter green). The coverage increases from top to bottom (0.50 ML, 0.75 ML, 1.00 ML, 1.50 ML); see ESI, section S3, for the complete spectra. Marked vibrations are shown in the insets of the panels (b) to (d), arrows point to the direction of motion. (b-f) Peak area  $A$  versus coverage  $\theta$  for (b) C-C stretching vibrations at  $1477\text{ cm}^{-1}$  (red) and  $1444\text{ cm}^{-1}$  (orange), (c) C-Cl stretching vibrations at  $1078\text{ cm}^{-1}$  (lighter green) and  $1084\text{ cm}^{-1}$  (darker green) and (d) C-H deformation vibration at  $1068\text{ cm}^{-1}$  (purple) and  $1022\text{ cm}^{-1}$  (pink). The solid and dashed lines on (e) Cu(111) (squares) and (f) Cu(110) (circles) are linear fits to the data. Insets in (e,f) are magnifications of the thresholds. (g,h) Scheme of the different adsorption orientations on (g) Cu(111) and (h) Cu(110) with P for parallel, PT for partially, and  $\text{CT}_{\downarrow}$  for completely tilted adsorption orientation. Note that the pictured angles of the molecules do not represent exact values.

stretching vibration at  $1478\text{ cm}^{-1}$  (Fig. 3b, red) is only detectable above the second threshold. The reason is that the C-C stretching vibration and the C-Cl stretching vibration change their dipole along the C-X bond, while the C-H deformation vibration and the other C-C stretching vibration change it at some angle (Fig. 1b). Thus, PT corresponds to a tilt around the C-X bond. The two different tilted orientations for chlorobenzene, as opposed to only one for bromobenzene, demonstrate that the surface structure and the halogen influences the adsorption orientation.

Having pinpointed differences between bromo- and chlorobenzene, we now discuss fluorobenzene that differs from the other two in terms of intermolecular binding. It is less prone to form halogen bonds because of its less pronounced

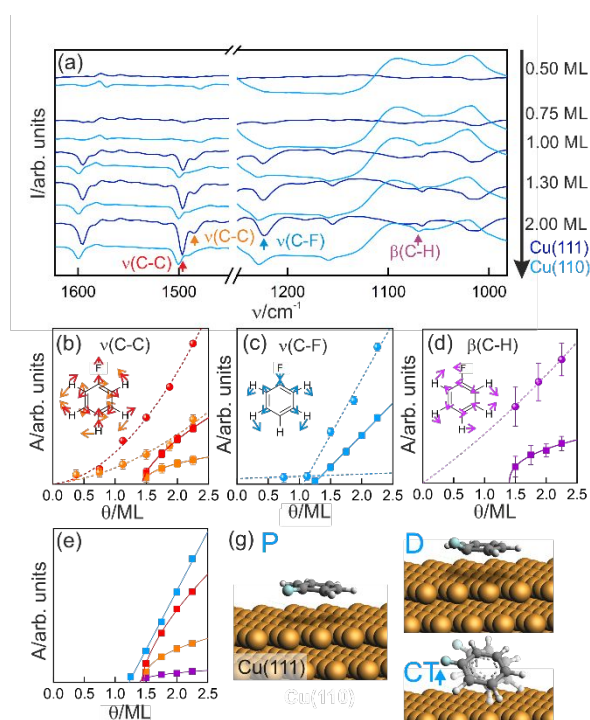


Fig. 4 Dependence of the adsorption orientation of fluorobenzene on surface structure: (a) RAIR spectra of fluorobenzene molecules on Cu(111) (darker blue) and Cu(110) (lighter blue). The coverage increases from top to bottom (0.50 ML, 0.75 ML, 1.00 ML, 1.30 ML, 2.00 ML); marked vibrations are shown in the insets of the panels (b) to (d); see ESI, section S3, for the complete spectra. (b-d) Peak area  $A$  versus coverage  $\theta$  for (b) C-C stretching vibrations at  $1500\text{ cm}^{-1}$  (red) and  $1470\text{ cm}^{-1}$  (orange), (c) C-F stretching vibrations at  $1222\text{ cm}^{-1}$  (blue), and (d) C-H deformation vibration at  $1068\text{ cm}^{-1}$  (purple). The solid and dashed lines on (e) Cu(111) (squares) and (f) Cu(110) (circles) are fits to the data (see text). (g,h) Scheme of the different adsorption orientations on (g), 1-3 | 5 Cu(111) and (h) Cu(110) with P for parallel, D for deformed, PT for partially tilted, and  $\text{CT}_{\uparrow}$  for completely tilted adsorption orientation. Note that the pictured angles of the molecules do not represent exact values.

$\sigma$ -hole, leading to a preference for hydrogen bonds<sup>35</sup>. For fluorobenzene, only the C-F stretching vibration at 1222 cm<sup>-1</sup> (blue) (Fig. 4c) rises linearly with coverage above thresholds at (1.22 ± 0.02) ML and (1.05 ± 0.05) ML for Cu(111) and Cu(110), respectively (Fig. 4). For Cu(110), the C-F stretching vibration

that all tilt angles increase continuously with coverage, apart from the C-F bond.

## Discussion

Our study of the orientation dependence of halogenated benzene molecules revealed a qualitative difference between the coverage dependence of fluorobenzene molecules to those of the other two halobenzene molecules and quantitative differences between the latter two molecules and the two surfaces. We relate these differences to an interplay between molecule-molecule and molecule-surface interactions, depending on the halogen and the surface structure.

On Cu(111), all three molecules adsorb at low coverages with their molecular plane parallel to the surface (Fig. 5a, P). Such a parallel adsorption orientation is a well-known phenomenon for molecules with  $\pi$ -systems<sup>37</sup>. It results from the high energy gain of the  $\pi$ -orbitals overlapping with the states of the metal. This gain is generally higher than the energy gain from the  $\pi$ - $\pi$ -stacking between the molecules, which would be expected to contribute to the energy gain in a tilted adsorption orientation<sup>38</sup>. In addition, the low corrugation of Cu(111) facilitates a stabilisation via intramolecular weak hydrogen and halogen bonds in a parallel adsorption orientation. Such intramolecular bonds resulted in self-organised clusters of chlorobenzene on Cu(111) that were calculated to be stable up to 120 K<sup>27</sup>, above the measurement temperature here. This cluster formation might be at the origin of the slightly different thresholds for chlorobenzene and bromobenzene. By DFT calculations and STM measurements, halogen-bond-stabilised tetramers and hexamers were determined to be the most stable cluster sizes for these two<sup>27</sup>. However, bromobenzene will be discussed in a forthcoming manuscript. The computational discussion and data (see ESI, section S4) supports the experimental determinations. DFT highlights the preferred hydrogen bonding, relatively low  $\pi$ - $\pi$ -stacking, and small tilting angle relative to Cu(111) for fluorobenzene and show how this induces largely parallel adsorption at lower coverages. For chlorobenzene and bromobenzene, the addition of halogen bonding to the molecule-molecule interactions coupled with a larger tilting angle to Cu(111) and stronger  $\pi$ - $\pi$ -stacking supports lower coverage tilting (see ESI, section S4). In contrast, fluorobenzene is adsorbed parallel to the surface up to almost the double coverage of 1.44 ML (Fig. 5a, blue). Note that 1.22 ML equals approximately the highest molecule density for parallel adsorbed molecules if all molecules adopted equivalent adsorption sites in a (4 × 4) superstructure. A denser packing in parallel adsorption orientation is possible if the C-F bonds of the molecules are slightly distorted (up to 1.44 ML, Fig. 5, D). The much higher threshold to a tilted orientation suggests a distinctly different interaction, stabilising an evenly distributed fluorobenzene layer, other than the clustered bromo- or chlorobenzene layers. As stated above, fluorobenzene differs in that it hardly forms halogen bonds, promoting a closed-packed layer in

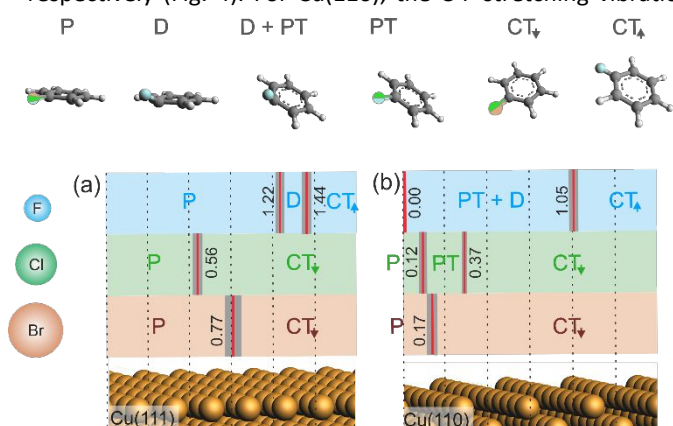


Fig. 5 Scheme of adsorption orientations of fluoro- (blue), chloro- (green), and bromobenzene (brown) on (a) Cu(111) and (b) Cu(110) vs coverage  $\theta$ . Determined thresholds are marked by red lines, with their error bars indicated in grey. Ball-and-stick models on top depict the adsorption orientations of the molecules.

increases linearly below and above its threshold with two distinct slopes. Thus, only for the C-F bond on Cu(111), the simple change from parallel to partially tilted at a threshold holds (P and PT + D in Fig. 4g). In contrast to chlorobenzene, the molecule is deformed with the C-F bond tilted out-of-plane. Furthermore, it is the fluorine atom that points away from the surface, as calculated<sup>36</sup>.

The coverage dependence of the other vibrational modes differs qualitatively on the two surfaces. On Cu(111), the areas increase sublinearly, fitted best by

$$y = A \cdot (x - B)^C, C < 1 \quad (1)$$

Fitting eq. 1 to the data recorded on Cu(111) leads to a common intersection of all fits with the x-axis at a threshold of (1.44 ± 0.02) ML (Fig. 4e), higher than the threshold of the C-F stretching vibration. Above this second threshold, all bonds, ring, C-F, and C-H, are tilted. The sublinear dependence results most likely from a lowering of the tilt angle of already adsorbed molecules.

The change in adsorption orientation follows an entirely different trend on Cu(110). Here, the area increases superlinearly, fitted best by a polynomial of second-order:

$$y = a + b \cdot x + c \cdot x^2 \quad (2)$$

Fitting eq. 2 to the data recorded on Cu(110) leads to a common intersection of all fits with the x-axis at 0 ML (Fig. 4f). Therefore, the first fluorobenzene molecules adsorb with all their bonds tilted to the Cu(110) surface (Fig. 4h). Furthermore, the superlinear increase in intensity suggests

parallel adsorption orientation to much higher coverages than chloro- or bromobenzene.

In contrast, only very few molecules adsorb parallel on Cu(110); for fluorobenzene, the threshold is even at 0 ML. The low amount of parallel adsorbed molecules is attributed to some intrinsic surface defects for the other two. Thus, the energy gain of the  $\pi$ -orbitals overlapping with the metal states is less prominent for the adsorption orientation on Cu(110) than on Cu(111).

At higher coverage, additionally adsorbed molecules of all six systems adsorb in a completely tilted orientation. Consequently, no bond remains parallel to the surface because the space on the surface, for chloro- and bromobenzene, is insufficient for more parallel-adsorbed molecules between the clusters. The threshold of fluorobenzene to this completely-tilted orientation at 1.05 ML corresponds to a closely-packed layer with a  $c(3 \times 4)$  superstructure. However, this close-packed structure is only possible if the ring is partially tilted (PT) and the C-F bond distorted (D). In contrast to the other molecules, there is a change in the adsorption orientation of already adsorbed molecules. Since the electronegative fluorine atom weakens the substrate-molecule interaction<sup>36</sup>, the energy gain of the  $\pi$ -systems of the rings is of comparable strength such that the two interactions compete, leading to a tilt, starting at low coverage. With an increasing number of molecules, the optimisation of the two energies increases the bond angle of already adsorbed molecules (CT $\uparrow$ ).

On Cu(111), a continuous adsorption orientation change of the completely tilted molecules exists, however, diametrically to the change on Cu(110). We reason this change in angle on Cu(111) as follows: The first molecules which do not adsorb parallel maximise their interaction with the surface by adsorbing at a large tilt angle. Further molecules that cannot interact directly with the metal surface only gain energy via  $\pi$ - $\pi$  interaction with these molecules, thereby forcing them to a less tilted orientation.

Finally, we comment on the partially tilted (PT) adsorption orientation of chlorobenzene on Cu(110) between 0.12 ML and 0.37 ML. We relate these partially tilted molecules to molecules adsorbed at step edges with the C-Cl bond parallel to the step edge, but the ring tilted across it. These molecules are not detected on Cu(111) because of its smaller step density at similar preparation conditions. We relate this variation to a higher amount of step edges on Cu(110) than on Cu(111). The bromobenzene does not adopt such a partially tilted orientation due to the larger size of the bromine atom.

As discussed above, the subtle interplay between the molecule-molecule and molecule-surface interactions causes a large variety of bonding angles and thresholds. The knowledge of the adsorption orientation is essential to understand on-surface reactivity as it determines the accessibility of the radical or functional group that participates in the reactions. For instance, a change in orientation of 2-iodoethanol on Pt(111) altered the product<sup>39</sup>. Likewise, the yield of graphene synthesis depends on the orientation of the reactants<sup>40</sup>. This becomes even more important for multi-substituted molecules. Our study demonstrated that a proper combination

of substituent, surface structure, and coverage could serve to optimize reactant orientation.

## Conclusions

In conclusion, we systematically explored the influence of the halogen atoms and the surface structure on the coverage dependence of the adsorption orientation of halogenated benzene molecules. Both parameters are essential for the coverage-dependent adsorption orientation, which vary from completely parallel via partially tilted around the C-X bond and distorted to completely tilted. The thresholds of the adsorption orientations also vary across the systems.

Because of differences in  $\sigma$ -hole depth, the fluorobenzene behaves differently to bromo- and chlorobenzene. Fluorobenzene has a preference for weak hydrogen bonding while chlorobenzene and bromobenzene integrate halogen bonding into their molecule-molecule interactions. Such variations reflect the disparate interplay of intramolecular and molecular-surface interactions controlled by the surface and the substituent. This is of utmost importance, especially for the field of on-surface synthesis like Ullmann coupling, where halogenated hydrocarbons on copper surfaces are prevalent. The knowledge of the substituent, the coverage and the surface structure leading to different adsorption orientations helps to control product formation in on-surface synthesis, paving the route to higher efficiency or less harsh reaction conditions.

## Conflicts of interest

There are no conflicts to declare.

## Acknowledgements

This work was supported by the Research Training group 'Confinement-controlled Chemistry', funded by the Deutsche Forschungsgemeinschaft (DFG) under Grant GRK2376/331085229 and the US National Science Foundation CHE-2108597. We thank Prashant Srivastava for providing STM images and Ting-Chieh Hung for providing LEED spectra of the pristine surface.

## Notes and references

§ Note that the extrapolated threshold of 0.12 ML is below the detection limit of our set-up.

- 1 S. Zarra, D. M. Wood, D. A. Roberts and J. R., Nitschke, Molecular containers in complex chemical systems. *Chem. Soc. Rev.*, 2015, **44**, 419-432.
- 2 F. Cheng, W. Ji, L. Leung, Z. Ning, J. C. Polanyi and C. Wang, How adsorbate alignment leads to selective reaction. *ACS Nano*, 2014, **8**, 8669-8675.
- 3 M. Müller, J. Henzl and K. Morgenstern, Confinement of a three-dimensional organic molecule to two dimensions on a surface. *Chem. Phys. Lett.*, 2019, **738**, 136906.

- 4 R. Lindner and A. Kühnle, On-surface reactions. *Chem. Phys. Chem.*, 2015, **16**, 1582-1592.
- 5 Q. Shen, H. Gao and H. Fuchs, Frontiers of on-surface synthesis: from principles to applications. *Nano Today*, 2017, **13**, 77-96.
- 6 L. Grill, M. Dyer, L. Lafferentz, M. Persson, M. V. Peters and S. Hecht, Nano-architectures by covalent assembly of molecular building blocks. *Nature Nanotechnology*, 2007, **2**, 687-691.
- 7 J. Cai, P. Ruffieux, R. Jaafar, M. Bieri, T. Braun, S. Blankenburg, M. Muoth, A. P. Seitsonen, M. Saleh, X. Feng, K. Müllen and R. Fasel, Atomically precise bottom-up fabrication of graphene nanoribbons. *Nature*, 2010, **466**, 470-473.
- 8 X. Zhang, Q. Zeng and C. Wang, On-surface single molecule synthesis chemistry: a promising bottom-up approach towards functional surfaces. *Nanoscale*, 2013, **5**, 8269-8287.
- 9 G. Galeotti, M. Di Giovannantonio, J. Lipton-Duffin, M. Ebrahimi, S. Tebi, A. Verdini, L. Floreano, Y. Fagot-Revurat, D. Perepichka and F. Rosei, The role of halogens in on-surface Ullmann polymerization. *Faraday Discuss.*, 2017, **204**, 453-469.
- 10 F. Ullmann and J. Bielecki, Über synthesen in der Biphenylreihe. *Ber. Dtsch. Chem. Ges.*, 1901, **34**, 2174-2185.
- 11 M. Xi and B. E. Bent, Iodobenzene on Cu(111): formation and coupling of adsorbed phenyl groups. *Surf. Sci.*, 1992, **278**, 19-32.
- 12 M.-T. Nguyen, C. A. Pignedoli and D. Passerone, An ab initio insight into the Cu(111)-mediated Ullmann reaction. *Phys. Chem. Chem. Phys.*, 2011, **13**, 154-160.
- 13 S. Clair and D. G. de Oteyza, Controlling a chemical coupling reaction on a surface: tools and strategies for on-surface synthesis. *Chem. Rev.*, 2019, **119**, 4717-4776.
- 14 L. Dong, P. N. Liu and N. Lin, Surface-activated coupling reactions confined on a surface. *acc. Chem. Res.*, 2015, **48**, 2765-2774.
- 15 Z. Chen, T. Lin, L. Zhang, B. Xiang, H. Xu, F. Klappenberger, J. V. Barth, S. Klyatskaya and M. Ruben, Surface-dependent chemoselectivity in C-C coupling reactions. *Angew. Chem. Int. Ed.*, 2019, **58**, 8356-8361.
- 16 H. Walch, R. Gutzler, T. Sirtl, G. Eder and M. Lackinger, Material- and orientation-dependent reactivity for heterogeneously catalyzed carbon-bromine bond homolysis. *J. Phys. Chem. C*, 2010, **114**, 12604-12609.
- 17 X. Zhang, D. Luo, H. Zhang, D. Y. Hwang, S. O. Park, B.-W. Li, M. Biswal, Y. Jiang, Y. Huang, S. K. Kwak, Ch. W. Bielawski and R. S. Ruoff, Effect of copper substrate surface orientation on the reductive functionalization of graphene. *Chem. Mater.*, 2019, **31**, 8639-8648.
- 18 M. X. Yang, M. Xi, H. Yuan, B. E. Bent, P. Stevens and J. M. White, NEXAFS studies of halobenzenes and phenyl groups on Cu(111). *Surf. Sci.*, 1995, **341**, 9-18.
- 19 A.F. Lee, R.M. Lambert, A. Goldoni, A. Baraldi and G. Paolucci, On the coverage-dependent adsorption geometry of benzene adsorbed on Pd(111): a study by fast XPS and NEXAFS. *J. Phys. Chem. B*, 2000, **104**, 11729-11733.
- 20 W. -K. Chen, M. -J. Cao, S. -H. Liu, Y. Xu and J. -Q. Li, On the coverage-dependent orientation of benzene adsorbed on Cu(100): a density functional theory study. *Chem. Phys. Lett.*, 2005, **407**, 414-418.
- 21 M. Xi, M.X. Yang, S. Jo and B.E. Bent, Benzene adsorption on Cu(111): formation of a stable bilayer. *J. Chem. Phys.*, 1994, **101**, 9122-9131.
- 22 S. Attia and S. Schauer mann, Coverage-dependent adsorption geometry of acetophenone on Pt(111). *J. Phys. Chem. C*, 2020, **124**, 557-566.
- 23 K. Boom, F. Stein, St. Ernst and K. Morgenstern, Coverage-induced conformational selectivity. *J. Phys. Chem. C*, 2017, **121**, 20254-20258.
- 24 A. Ulman, Formation and structure of self-assembled monolayers. *Chem. Rev.*, 1996, **96**, 1533-1554.
- 25 A. Michaelides and K. Morgenstern, Ice nanoclusters at hydrophobic metal surfaces. *Nature Mat.*, 2007, **6**, 597-601.
- 26 Y. Lu, S. Zhang, C. Peng and H. Liu, Interplay between halogen and hydrogen bonds in 2D self-assembly on the gold surface: a first-principles investigation. *J. Phys. Chem. C*, 2017, **121**, 24707-24720.
- 27 C. Bertram, D. P. Miller, Chr. Schunke, I. Kemeny, M. Kimura, U. Bovensiepen, E. Zurek and K. Morgenstern, The interplay of halogen and weak hydrogen bonds in the formation of magic nanoclusters on surfaces. *J. Phys. Chem. C*, 2021, *in print*.
- 28 G. Cavallo, P. Mentrangolo, R. Milani, T. Pilati, A. Priimagi, G. Resnati and G. Terraneo, The halogen bond. *Chem. Rev.*, 2016, **116**, 2478-2601.
- 29 K. J. Donald, B. K. Wittmaack and C. Crigger, Tuning  $\sigma$ -holes: charge redistribution in the heavy (group 14) analogues of simple and mixed halomethanes can impose strong propensities for halogen bonding. *J. Phys. Chem. A*, 2010, **114**, 7213-7222.
- 30 J. Tschakert, Q. Zhong, D. Martin-Jimenez, J. Carracedo-Cosme, C. Romero-Muñiz, P. Henkel, T. Schlöder, S. Ahles, D. Mollenhauer, H. A. Wegner, P. Pou, R. Pérez, A. Schirmeisen and D. Ebeling, Surface-controlled reversal of the selectivity of halogen bonds. *Nat. Commun.*, 2020, **11**, 5630.
- 31 R. G. Greenler, D. R. Snider, D. Witt and R. S. Sorbello, The metal-surface selection rule for infrared spectra of molecules adsorbed on small metal particles. *Surf. Sci.*, 1982, **118**, 415-428.
- 32 Y. Wang, A. Glenz, M. Muhler and Ch. Wöll, A new dual-purpose ultrahigh vacuum infrared spectroscopy apparatus optimized for grazing-incidence reflection as well as for transmission geometries. *Rev. Sci. Instrum.*, 2009, **80**, 113108.
- 33 D. H. Whiffen, Vibrational frequencies and thermodynamic properties of fluoro-, chloro-, bromo-, and iodobenzenes. *J. Chem. Soc.*, 1956, 1350-1356.
- 34 D. Steele, The absolute intensities of infrared adsorption bands. *Q. Rev. Chem. Soc.*, 1964, 21-44.
- 35 V. R. Thalladi, H.-C. Weiss, D. Bläser, R. Boese, A. Nangia and G. R. Desiraju, C-H...F interactions in the crystal structures of some fluorobenzenes. *J. Am. Chem. Soc.*, 1998, **120**, 8702-8710.
- 36 L. A. Zotti, G. Teobaldi, K. Palotas, W. Ji, H. -J. Gao and W. A. Hofer, Adsorption of benzene, fluorobenzene and meta-difluorobenzene on Cu(110): a computational study. *J. Comput. Chem.*, 2008, **29**, 1589-1595.
- 37 S. M. Barlow and R. Raval, Complex organic molecules at metal surfaces: bonding, organisation and chirality. *Surf. Sci. Rep.*, 2003, **50**, 201-341.
- 38 T. Dretschkow, T. Wandlowski, K. Wandelt (Eds.) and S. Thurgate (Eds.), *solid-liquid interfaces*, Springer Verlag, Berlin Heidelberg, 2003, page 259-321.
- 39 M. B. Griffin, S. H. Pang, and J. W. Medlin, Surface chemistry of 2-iodoethanol on Pd(111): orientation of surface-bound alcohol controls selectivity. *J. Phys. Chem. C*, 2012, **116**, 4201-4208.
- 40 F. Schulz, P. H. Jacobse, F. F. Canova, J. van der Lit, D. Z. Gao, A. van den Hoogenband, P. Han, R. J.M. Klein Gebbink, M.-E. Moret, P. M. Joensuu, I. Swart, and P. Liljeroth, Precursor geometry determines the growth mechanism in graphene nanoribbons. *J. Phys. Chem. C*, 2017, **121**, 2896-2904.

